Excitonic condensation of strongly correlated electrons: The case of $Pr_{0.5}Ca_{0.5}CoO_3$

Jan Kuneš* and Pavel Augustinský

Institute of Physics, Academy of Sciences of the Czech Republic, Cukrovarnická 10, 162 53 Praha 6, Czech Republic

(Received 6 May 2014; revised manuscript received 21 November 2014; published 4 December 2014)

We use a combination of dynamical mean-field model calculations and LDA + U material specific calculations to investigate the low temperature phase transition in the compounds from the $(Pr_{1-y}R_y)_xCa_{1-x}CoO_3$ (R = Nd, Sm, Eu, Gd, Tb, Y) family (PCCO). The transition, marked by a sharp peak in the specific heat, leads to an exponential increase of dc resistivity and a drop of the magnetic susceptibility, but no order parameter has been identified yet. We show that condensation of spin-triplet, atomic-size excitons provides a consistent explanation of the observed physics. In particular, it explains the exchange splitting on the Pr sites and the simultaneous Pr valence transition. The excitonic condensation in PCCO is an example of a general behavior expected in certain systems in the proximity of a spin-state transition.

DOI: 10.1103/PhysRevB.90.235112 PACS number(s): 71.35.Lk, 71.27.+a, 75.30.Fv

The $R_xA_{1-x}CoO_3$ (R = La, ..., and A = Ca, Sr, Ba) series exhibits a variety of phenomena including thermally and doping driven spin-state crossover, metal-insulator crossover, magnetic ordering or formation of nanoscopic inhomogeneities. The root causes of the rich physics are quasidegenerate Co 3*d* atomic multiplets and their interaction with the crystal lattice or doped charge carriers. The $(Pr_{1-y}R_y)_xCa_{1-x}CoO_3$ (R = Nd, Sm, Eu, Gd, Tb, Y) family is unique among the cobaltites. A decade ago, Tsubouchi *et al.* [1,2] observed a metal-insulator transition in $Pr_{0.5}Ca_{0.5}CoO_3$ associated with a drop of magnetic susceptibility and a sharp peak in the specific heat indicating the collective nature of the transition. Subsequently, the transition was observed in other PCCO materials with x and y in the ranges 0.2–0.5 and 0–0.3, respectively [3–5]. Despite the evidence for a continuous, or very weakly first order, phase transition and the experimental effort [6], no long-range order could be identified. The PCCO materials in this respect resemble the much famous hidden order prototype URu_2Si_2 [7]. An important step towards understanding of the transition in PCCO was made by the observation of the $Pr^{3+} \rightarrow Pr^{4+}$ valence transition which takes place simultaneously [6,8]. Another clue to the nature of the PCCO hidden order is the exchange splitting of the Pr^{4+} Kramers ground state in the absence of ordered magnetic moments [4,6,9].

The basic features to be captured by a theory of the PCCO hidden order are (i) the substantial increase of resistivity below the transition temperature T_c, (ii) the sharp peak in the specific heat at T_c, (iii) the drop of the magnetic susceptibility and the departure from the Curie-Weiss behavior of the Co moments below T_c, (iv) the Pr valence transition, and (v) the exchange splitting of the Pr^{4+} Kramers doublet in the absence of ordered magnetic moments. More subtle effects include the increase of T_c with pressure [3], the lattice response consisting primarily in the reduction of the Co-O-Co angle below T_c [3], and the apparent softness of the exchange field on Pr and the lack of a clear x-ray signature of the spin-state transition [6,10].

In this paper we explain the physics of PCCO by the formation of excitonic condensate (EC). Motivated by the observation of excitonic instability of correlated electrons close to a spin-state transition [11], we have performed two types of investigations. First, we have studied the EC phase in a minimal model using the dynamical mean-field theory (DMFT) [12] and calculated temperature T dependencies of the various physical quantities across the transition. Second, we have obtained a $T = 0$ EC solution for PCCO using the density-functional LDA + U method [13,14].

The two-orbital Hubbard model (1) captures the competition between the atomic high-spin (HS) and low-spin (LS) states and thus provides a minimal description of a solid with a spin-state transition:

$$H = \frac{\Delta}{2}\sum_{i,\sigma}\left(n^a_{i\sigma} - n^b_{i\sigma}\right) + \sum_{\langle ij\rangle,\sigma}\left(t_a a^\dagger_{i\sigma}a_{j\sigma} + t_b b^\dagger_{i\sigma}b_{i\sigma}\right) + U\sum_{i,\alpha=a,b} n^\alpha_{i\uparrow}n^\alpha_{i\downarrow} + U'\sum_{i,\sigma} n^a_{i\sigma}n^b_{i\bar{\sigma}} + (U'-J)\sum_{i,\sigma} n^a_{i\sigma}n^b_{i\sigma}. \quad (1)$$

Here $a^\dagger_{i\sigma}$, $b^\dagger_{i\sigma}$ are the creation operators of fermions with spin $\sigma = \uparrow,\downarrow$ in orbitals a and b on the site i of a square lattice, and $n^{a,b}_{i\sigma}$ are the corresponding occupation number operators. The DMFT calculations using the impurity solver of Werner *et al.* [15] were performed for the interaction parameters $U' = U - 2J$, $U = 4$ and $J = 1$, the hopping amplitudes $t_a = 0.4118$ and $t_b = -0.1882$, and the crystal field $\Delta = 3.40$, assuming eV to be the unit of energy. Details can be found in the Supplemental Material (SM) [16]. The model captures the basic features of perovskite cobaltites: nearly degenerate LS and HS atomic states, the energy scales of the bandwidths and the interaction strength, a band gap/overlap being much smaller than the bandwidths, and the dominant Co-Co nearest-neighbor hopping on a bipartite lattice preserving the orbital flavor. The main approximation consists in neglecting the actual orbital degeneracy of the *d* shell.

Linear response calculations [11] predicted the model to exhibit excitonic instability in the magnetic channel. The spin-triplet EC order parameter for the model with the SU(2) symmetric interaction is a vector $\phi_i = \sum_{\alpha\alpha'=\uparrow,\downarrow}\boldsymbol{\sigma}_{\alpha\alpha'}\langle a^\dagger_{i\alpha}b_{i\alpha'}\rangle$ [17,18], where $\boldsymbol{\sigma}$ are the Pauli matrices. For the density-density interaction of Hamiltonian (1) ϕ is constrained to the xy plane. First, we investigate the model at a fixed particle density n of two electrons per atom. In Fig. 1(a) we show the evolution of the order parameter ϕ, which was chosen to point in the

*kunes@fzu.cz

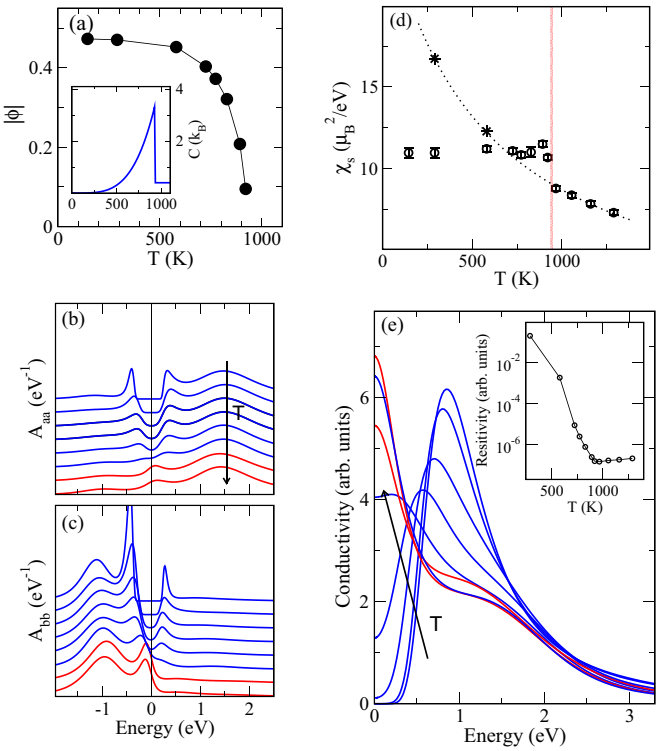

FIG. 1. (Color online) The DMFT results for fixed particle density $n = 2$. (a) The magnitude of the order parameter $|\phi(T)|$. The inset shows specific heat $C(T)$. (b), (c) The spectral functions $A_{aa}(\omega)$ and $A_{bb}(\omega)$, respectively, at $T = 1160, 968, 921, 892, 829, 725, 580, 290$ K. (blue curves for $T < T_c$, the red ones for $T > T_c$). The arrow marks the direction of increasing temperature. (e) The corresponding optical conductivity. The inset shows the dc resistivity. (d) The spin susceptibility $\chi_S(T)$ (circles with error bars) and $\chi_S(T)$ of the constrained normal phase solutions (dotted line).

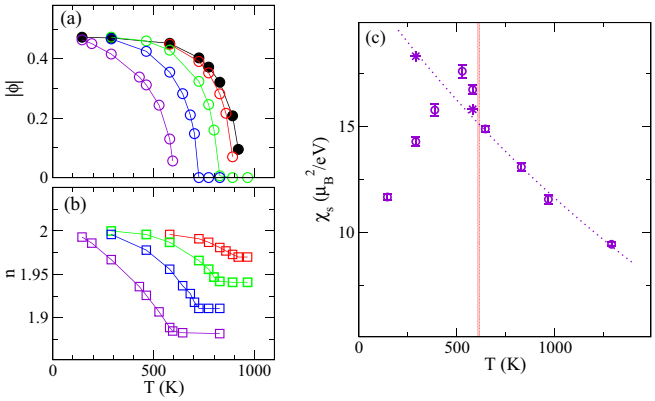

FIG. 2. (Color online) (a) The magnitude of the order parameter $|\phi(T)|$ for various fixed chemical potentials (The $|\phi(T)|$ for $n = 2$ taken from Fig. 1 is marked by black circles). (b) The corresponding particle densities n as functions of temperature. The curves correspond to the doping of 0.03 (red), 0.06 (green), 0.09 (blue), and 0.12 (violet) holes per atom in the normal phase. (c) The susceptibility $\chi_S(T)$ for the 0.12 hole doping. The symbols have the same meaning as in Fig. 1.

x direction. The inset shows the specific heat per atom with a typical mean-field shape. Nonzero ϕ_x is connected to the appearance of a spin off-diagonal (anomalous) element of the self-energy (see the SM for an example), which opens a gap in the one-particle spectra, Figs. 1(b) and 1(c). The gap opening is reflected in the behavior of the optical conductivity, Fig. 1(e). The Drude peak is suppressed below T_c and the dc resistivity, shown in the inset, grows exponentially upon cooling. While there are no ordered moments below T_c the spin susceptibility $\chi_S(T)$, Fig. 1(d), is strongly affected by the EC transition. In the high-T normal phase, thermally excited HS states lead to Curie-Weiss $\chi_S(T)$. While HS states are present in the EC phase, they are not free. The anomalous self-energy gives rise to an on-site hybridization between the LS and HS states which results in a T-independent Van Vleck $\chi_S(T)$. The sign of the change of $\chi_S(T)$ at T_c depends on details of the system, in particular, a reduction of T_c by doping, as discussed below, leads to the same sign of $\chi_S(T)$ change as in the experiment. The fact that HS population does not vanish in the EC phase can explain the absence of changes in the x-ray spectra [6] typical for the spin-state transition.

The Co bands of PCCO differ from the above model in an important aspect. They are hole doped in the normal state and their filling changes due to the $Pr^{3+} \rightarrow Pr^{4+}$ valence transition. The isostructural valence transition points to a near degeneracy of the f^2 and f^1 states of the Pr $4f$ shell. The Pr ions therefore act as a charge reservoir providing electrons to the Co bands and can be modeled by fixing the chemical potential μ in the above calculations. In the following we present model results obtained with fixed μ. The particle density $n(T)$ in the normal phase is very weakly T dependent and thus can be used to label the different choices of μ. In Fig. 2 we show $|\phi|$ for dopings between 0.03 and 0.12 holes per atom. Doping away from the half filling leads to a reduction of T_c. Unlike in the normal phase, $n(T)$ varies considerably below T_c. With decreasing T the system draws electrons from the reservoir, a process controlled by competition between the condensation energy, favoring an equal number of a electrons and b holes, and the energy of adding electrons from the reservoir. The present theory thus provides a simple connection between the Pr valence change and the EC transition, and explains why these happen simultaneously [6]. The evolution of the one-particle spectra at fixed μ (see SM) is similar to Figs. 1(b) and 1(c) although the spectrum becomes fully gapped only at half filling. The behavior of the $\chi_S(T)$ for fixed μ is shown in Fig. 2(c).

The model calculations capture the features (i)–(iv). The (i)–(iii) are generic features of the EC transition in a half-filled system that survive to a doped material kept at fixed μ. The feature (iv) is accounted for by treating the Pr ions as a charge reservoir for the Co bands. There are several limitations associated with the DMFT method as well as the model itself. The mean-field character of the method is responsible for the extremely asymmetric peak in the specific heat $C(T)$ as well as the kink in $n(T)$ at T_c. The experimental $C(T)$ and $n(T)$ [6] do not exhibit this pronounced asymmetry which can be explained by short-range EC correlations above T_c. The model also ignores the change of the lattice below T_c consisting in bending of Co-O-Co without changing the Co-O bond length. It enhances the e_g-t_{2g} hopping, which provides a positive feedback to the EC transition. The transition with the lattice

taken into account is therefore expected to be sharper, perhaps even weakly first order, than in a purely electronic model.

In order to test the EC scenario in a more realistic setting and to address the feature (v) we have performed a material specific calculation using the LDA + U method. It roughly amounts to a $T = 0$ static mean-field solution for the Hamiltonian including all electronic orbitals, the experimental crystal structure, and unrestricted hopping. Such a calculation can answer the question as to whether the EC order in PCCO is plausible. The ability of the method to capture complex long-range orders was demonstrated by Cricchio *et al.* [19,20] on URu_2Si_2 and LaFeAsO.

Before presenting the results for the orthorhombic PCCO structure we discuss symmetry aspects of the EC in a cubic crystal. As in the model, the Hund's coupling selects the spin part of the order parameter to be a triplet. The orbital part describes a pair of an e_g electron and a t_{2g} hole, which transforms as an $E_g \times T_{2g} = T_{2g} + T_{1g}$ representation under the cubic symmetry operations. General considerations suggest that only T_{1g} pairs, $d_{xy} \otimes d_{x^2-y^2}$, $d_{xz} \otimes d_{x^2-z^2}$, and $d_{yz} \otimes d_{y^2-z^2}$ can condense. The electrons and holes forming a T_{1g} pair have large hopping amplitudes along the same "in-plane" directions, while the electrons and holes forming a T_{2g} pair of the form $d_{xy} \otimes d_{z^2}$ maximize their hoppings in mutually perpendicular directions, which is detrimental to the condensation. Moreover, the electron-hole bonding is stronger for a T_{1g} than for a T_{2g} pair. The EC order in a cubic symmetry is thus characterized by nine parameters ϕ^α_β, where α runs over the three Cartesian spin components and β over three T_{1g} orbital components. The anomalous part of the Co $3d$ occupation matrices in terms of ϕ^α_β can be found in the SM. We have verified that the numerical LDA + U solutions have these symmetry properties by performing a series of calculations in a cubic perovskite structure, which will be reported separately.

The LDA + U calculations for PCCO were performed in the structure of Ref. [8] with a unit cell containing four Co sites. On-site interaction parametrized with $U = 4$ eV and $J = 1$ eV was assumed for the Co $3d$ shells. All Pr ions were assumed to be in the 4+ state, which was enforced by constraining the f^1 occupancy in so-called core treatment of the Pr $4f$ states. We found a stable EC solution with the total energy 230 meV per formula unit lower than the normal state one. The EC was detected by the appearance of spin-triplet terms in the Co $3d$ occupation matrix. Reflecting the approximate cubic symmetry of the Co sites, the orbital part of the anomalous terms is dominated by the T_{1g} components. The order parameter of the present solution can be written as a product $\phi^\alpha_\beta = \varphi_\beta \otimes e^\alpha_S$ of a spin vector e^α_S pointing in arbitrary direction, but common to all Co sites, and an orbital pseudovector φ_β, shown in Table I. The product form of ϕ^α_β with real elements results in the collinear spin-density distribution shown in Fig. 3. Inspection of φ_β for symmetry related Co sites reveals an odd parity of the order parameter under the mirror image σ_h by a plane perpendicular to the c axis. The EC solution does not exhibit ordered local moments ($|\mathbf{m}| < 0.03\mu_B$ inside WIEN2K atomic spheres). The orbital resolved spectral functions can be found in the SM.

Next, we address feature (v), the exchange splitting of the Kramers ground state of the Pr^{4+} ion. The EC with real ϕ^α_β breaks the time reversal symmetry. However, we have to show that this symmetry breaking is felt by the Pr moments. Microscopic analysis based on a multiband Kondo impurity model can be found in the SM. Here we use direct numerical calculation. To estimate the exchange splitting arising from the $4f$-ligand hybridization we diagonalize the Kohn-Sham Hamiltonian of the EC solution with Pr $4f$ orbitals included (with E_{4f} inside the gap). This approach mimics the effect of the $f^1 \to f^2\underline{L}$ denotes a ligand hole virtual excitation [21]. The calculated $4f$ spectrum is shown in Fig. 4. The exchange splitting induced by the EC order is clearly visible on top of the dominant spin-orbit and crystal-field splitting. The $4f$ spin-orbit coupling (SOC) is crucial. As shown in the inset of Fig. 4, the EC order that is odd under the mirror image σ_h does not couple to individual $4f$ crystal-field states (without $4f$ SOC), which are either σ_h odd or σ_h even. It is only the SOC, which mixes the σ_h-odd and σ_h-even $4f$ functions and thus allows the exchange splitting (see the SM for more detail). The exchange splitting of the order of 10 meV overestimates the experimental values of a few Kelvin. This is not surprising given the approximations involved, in particular the mean-field treatment of the Pr $4f$ shell which in reality presents a complicated quantum impurity problem.

Spin-triplet excitonic condensation provides a comprehensive description of the phase transition observed in the PCCO series. In particular, we are not aware of an alternative theory of the exchange splitting of the Pr $4f$ states. It is not clear at the moment why the excitonic condensation takes place in PCCO, but not in other cobaltites close to stoichiometric filling, e.g., $LaCoO_3$. The answer is related to the nature of the lowest excited states of the Co ion. The $S = 2$ states tend

TABLE I. The orbital part of the EC oder parameter on the four Co atoms in the unit cell of PCCO with respect to the local coordinates tied to the CoO_6 octahedra. The sites 1,2 and 3,4 are connected by σ_h symmetry.

	1	2	3	4
φ_{yz}	0.182	0.182	0.216	0.216
φ_{zx}	0.228	0.228	−0.212	−0.212
φ_{xy}	−0.071	0.071	−0.093	0.093

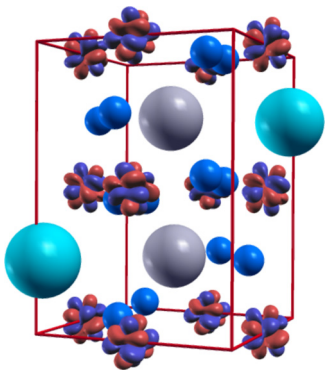

FIG. 3. (Color online) The distribution of the collinear spin density (red and blue correspond to positive and negative signs respectively) around Co atoms in PCCO with O (blue), Ca (light blue), and Pr (gray).

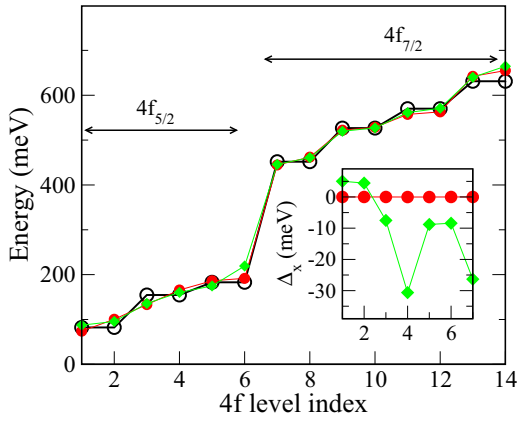

FIG. 4. (Color online) The spectrum of the Pr $4f$ states: no EC order (black), the self-consistent LDA + U solution with the σ_h-odd order parameter (red), and with an artificial order parameter of the same magnitude containing a σ_h-even contribution (green). The inset shows the exchange splitting of the $4f$ levels for the same order parameters when spin-orbit coupling is not included.

to form a solid lattice on the LS background [22,23], while $S = 1$ states are susceptible to the excitonic condensation. A phase separation is another competing alternative in the doped systems.

The low-temperature phase of PCCO is an example of complex multipole order which is detected only through its indirect effects. Unlike URu_2Si_2 or LaOFeAs where the hidden order and nematicity arise from Fermi surface nesting [24,25], PCCO are strongly correlated oxides and the transition here is closer to condensation of preexisting composite bosons. The present mechanism of the excitonic condensation is quite general and therefore it should be possible to find it in other materials exhibiting singlet-triplet spin-state transitions [26].

We acknowledge numerous discussions with Z. Jirák, P. Novák, A. Kauch, and D. Vollhardt. The work was supported through the research unit FOR 1346 of the Deutsche Forschungsgemeinschaft and the Grant No. 13-25251S of the Grant Agency of the Czech Republic.

[1] S. Tsubouchi, T. Kyômen, M. Itoh, P. Ganguly, M. Oguni, Y. Shimojo, Y. Morii, and Y. Ishii, Phys. Rev. B **66**, 052418 (2002).
[2] S. Tsubouchi, T. Kyômen, M. Itoh, and M. Oguni, Phys. Rev. B **69**, 144406 (2004).
[3] T. Fujita, T. Miyashita, Y. Yasui, Y. Kobayashi, M. Sato, E. Nishibori, M. Sakata, Y. Shimojo, N. Igawa, Y. Ishii *et al.*, J. Phys. Soc. Jpn. **73**, 1987 (2004).
[4] J. Hejtmánek, E. Šantavá, K. Knížek, M. Maryško, Z. Jirák, T. Naito, H. Sasaki, and H. Fujishiro, Phys. Rev. B **82**, 165107 (2010).
[5] V. Hardy, F. Guillou, and Y. Brard, J. Phys.: Condens. Matter **25**, 246003 (2013).
[6] J. Hejtmánek, Z. Jirák, O. Kaman, K. Knížek, E. Šantavá, K. Nitta, T. Naito, and H. Fujishiro, Eur. Phys. J. B **86**, 305 (2013).
[7] J. A. Mydosh and P. M. Oppeneer, Rev. Mod. Phys. **83**, 1301 (2011).
[8] K. Knížek, J. Hejtmánek, P. Novák, and Z. Jirák, Phys. Rev. B **81**, 155113 (2010).
[9] K. Knížek, J. Hejtmánek, M. Maryško, P. Novák, E. Šantavá, Z. Jirák, T. Naito, H. Fujishiro, and C. de la Cruz, Phys. Rev. B **88**, 224412 (2013).
[10] J. Herrero-Martín, J. L. García-Muñoz, K. Kvashnina, E. Gallo, G. Subías, J. A. Alonso, and A. J. Barón-González, Phys. Rev. B **86**, 125106 (2012).
[11] J. Kuneš and P. Augustinský, Phys. Rev. B **89**, 115134 (2014).
[12] A. Georges, G. Kotliar, W. Krauth, and M. J. Rozenberg, Rev. Mod. Phys. **68**, 13 (1996).
[13] A. B. Shick, A. I. Liechtenstein, and W. E. Pickett, Phys. Rev. B **60**, 10763 (1999).
[14] P. Blaha, K. Schwarz, G. K. H. Madsen, D. Kvasnicka, and J. Luitz, WIEN2K, *An Augmented Plane Wave + Local Orbitals Program for Calculating Crystal Properties* (Karlheinz Schwarz, Technische Universität Wien, Austria, 2001).
[15] P. Werner, A. Comanac, L. de' Medici, M. Troyer, and A. J. Millis, Phys. Rev. Lett. **97**, 076405 (2006).
[16] See Supplemental Material at http://link.aps.org/supplemental/10.1103/PhysRevB.90.235112 for the details of the DMFT calculations, an example of the anomalous Green's function and self energy, and a discussion of the excitonic order parameter for *a d* shell in cubic environment.
[17] T. Kaneko, K. Seki, and Y. Ohta, Phys. Rev. B **85**, 165135 (2012).
[18] B. I. Halperin and T. M. Rice, *The Excitonic State at the Semiconductor-Semimetal Transition* (Academic Press, New York, 1968), Vol. 21, p. 115.
[19] F. Cricchio, F. Bultmark, O. Grånäs, and L. Nordström, Phys. Rev. Lett. **103**, 107202 (2009).
[20] F. Cricchio, O. Grånäs, and L. Nordström, Phys. Rev. B **81**, 140403 (2010).
[21] P. Novák, K. Knížek, and J. Kuneš, Phys. Rev. B **87**, 205139 (2013).
[22] K. Knížek, Z. Jirák, J. Hejtmánek, P. Novák, and W. Ku, Phys. Rev. B **79**, 014430 (2009).
[23] J. Kuneš and V. Křápek, Phys. Rev. Lett. **106**, 256401 (2011).
[24] H. Ikeda, M. Suzuki, R. Arita, T. Takimoto, T. Shibauchi, and Y. Matsuda, Nat. Phys. **8**, 528 (2012).
[25] R. M. Fernandes, A. V. Chubukov, and J. Schmalian, Nat. Phys. **10**, 97 (2014).
[26] G. Khaliullin, Phys. Rev. Lett. **111**, 197201 (2013).